Measurements of ferrofluid surface tension in confined geometry

C. Flament,[1,2] S. Lacis,[2,3] J.-C. Bacri,[1,2] A. Cebers,[2,3] S. Neveu,[4] and R. Perzynski[1]
[1]Laboratoire d'Acoustique et d'Optique de la Matière Condensée, URA 800 associée au CNRS et à l'Université Paris 6, Tour 13, case 78, 4 place Jussieu, 75252 Paris cedex 05, France
[2]Université Paris 7, Unite de Formation et de Recherche de Physique, 2 place Jussieu, 75251 Paris Cedex 05, France
[3]Institute of Physics–Latvian Academy of Sciences, Salaspils 1, 2169 Riga, Latvia
[4]Laboratoire de Physico-Chimie Inorganique, URA associée au CNRS et à l'Université Paris 6, Bâtiment F, case 63, 4 place Jussieu, 75252 Paris cedex 05, France
(Received 18 September 1995)

Two methods of determination of the surface tension at the interface of a magnetic liquid and another fluid, in a confined two-dimensional geometry, are presented. The first is based upon a surface instability under the action of a vertical magnetic field and the second uses the deformation of a magnetic droplet in plane layer under the influence of a horizontal magnetic field. Theoretical calculations and experimental results are presented in both cases. Both determinations lead to comparable values of the surface tension $\sigma \approx 3$ mN m^{-1}.[S1063-651X(96)00205-X]

PACS number(s): 47.65.+a, 75.50.Mm, 68.10.−m

I. INTRODUCTION

Magnetic fluids (MFs) between two parallel plates (a Hele-Shaw cell) under the action of a perpendicular magnetic field present labyrinthine patterns due to the competition between the short-range attractive forces and the long-range repulsion forces [1–4]. Different features of these pattern formation phenomena are quite well understood theoretically [1–6]. For a quantitative comparison with the existing experimental data, the knowledge of the surface tension of the MF σ is crucial. Surface tension measurements *in situ* are useful in the study of the behavior of magnetic liquids in plane layers. For example, describing the behavior of magnetic stripe systems in the framework of the smectic analogy [6], curvature and compression elasticity constants depend on the magnetic field and also on σ. These elastic moduli can be determined from macroscopic experiments [7] and it is essential to know σ for a comparison with the theoretical predictions.

We turn here the analysis of two surface deformations in two dimensions into two genuine σ determinations under an external magnetic field. In our description, σ is supposed to be a field-independent constant. The self-consistency between the two kinds of σ determinations at different fields supports this usual hypothesis.

Since MF presents surface instabilities, classical methods for the determination of the surface tension under a magnetic field are difficult or even impossible to handle. Deformations of the free surface strongly disturb measurements with a Langmuir balance [8] or with ultrasonic waves [9]. Because both these methods use the surface instabilities for the determination of σ, they are the only ones to get σ for a MF under the influence of a magnetic field.

II. THEORETICAL BACKGROUND

Our two kinds of σ measurements are based on an analysis of the surface deformation of a MF in a two-dimensional (2D) geometry and under a magnetic field. In order to describe the competition between the magnetic forces and the capillary forces, let us introduce the magnetic Bond number, which is defined as $N_B = \mu_0 H_0^2 h / 2\sigma$ and represents the ratio of a magnetic pressure and a capillary pressure, where h is the thickness of the layer.

A. Normal field instability in plane layers

Instability phenomena at the interface between a MF and another fluid, under the influence of a magnetic field normal to the interface, are quite well known [10,11]. Previous studies have shown that the surface instability leads to peak formations. The wavelength of the surface deformation at the threshold value of the magnetic field strength is given by the capillary length of the fluids $\lambda_c = \lambda_0 = 2\pi\sqrt{\sigma/(\rho_1 - \rho_2)g}$. If the density difference between the two liquids is known, the measurement of the critical wavelength can be employed for the determination of σ. However, in the present case, the results of this 3D analysis cannot be directly employed because the critical wavelength λ_c of the free-surface deformation is comparable to that of the layer thickness. Consequently, the exact neutral curve of the instability taking into account the finite thickness of the layer is established.

The system is sketched in Fig. 1. Let us call $y = \xi(x)$ the

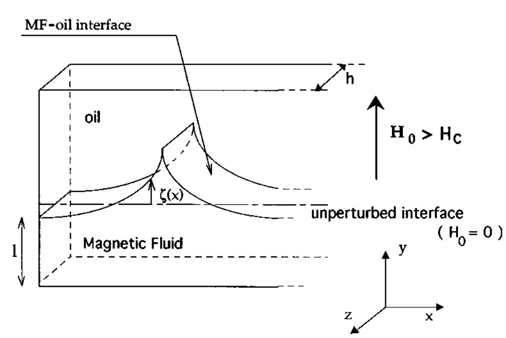

FIG. 1. Sketch of the Hele-Shaw cell with its axes in the peak instability experiment showing the invariant peak shape in the z direction.

equation of the free boundary and H_0 the external magnetic field perpendicular to the interface. The motion of the fluids in the Hele-Shaw approximation is described by the Darcy equation [5]

$$-\alpha\vec{v}-\vec{\nabla}p+\frac{\mu_0}{h}\int_{-h/2}^{+h/2}dz(\vec{M}\cdot\vec{\nabla})\vec{H}+\rho\vec{g}=\vec{0},\mathrm{div}(\vec{v})=0, \tag{1}$$

where the permeability α is given by the ratio $12\eta/h^2$, η is the viscosity, and $\vec{v}$ is the average local velocity of the fluids. Introducing a magnetic potential $\vec{H}=\vec{\nabla}\psi$ and due to the potentiality of the Hele-Shaw flow, the velocity is $\vec{v}=\vec{\nabla}\varphi$. We assume that the magnetization is along the external field and that the influence of the demagnetizing field is neglected. The Darcy equation for the MF (denoted by 1) can be written as

$$-\alpha_1\varphi_1-p_1+\frac{\mu_0}{h}\int_{-h/2}^{+h/2}dz\ M\ \frac{\partial\psi}{\partial y}+\rho_1\vec{g}\cdot\vec{r}=0. \tag{2}$$

The upper nonmagnetic fluid (denoted by 2) may be described by

$$-\alpha_2\varphi_2-p_2+\rho_2\vec{g}\cdot\vec{r}=0. \tag{3}$$

At the free boundary, we have the modified Laplace law in order to take into account the magnetic phenomena

$$p_1-p_2=\frac{\sigma}{R_c}-\frac{\mu_0}{2}(\vec{M}\cdot\vec{n})^2 \quad \text{with} \quad \frac{1}{R_c}=-\frac{\partial^2\zeta}{\partial x^2}=-\zeta'', \tag{4}$$

where σ is the surface tension between the fluids. In the stationary state (denoted by 0), for the flat interface we have

$$-\frac{\partial p_1^0}{\partial y}+\frac{\mu_0}{h}\int_{-h/2}^{+h/2}dz\ M\ \frac{\partial^2\psi^0}{\partial y^2}-\rho_1 g=0 \tag{5}$$

and

$$-\frac{\partial p_2^0}{\partial y}-\rho_2 g=0. \tag{6}$$

In the framework of a linear analysis, Eqs. (4)–(6) give, for the difference of the pressures on the unperturbed surface as a function of the interface displacement ζ,

$$\delta p_1-\delta p_2=-\sigma\zeta''+\zeta(\rho_1-\rho_2)g-\zeta\frac{\mu_0}{h}\int_{-h/2}^{+h/2}dz\ M\ \frac{\partial^2\psi^0}{\partial y^2}$$

and for the velocity potential

$$-\alpha_1\varphi_1+\alpha_2\varphi_2+\sigma\zeta''-\zeta(\rho_1-\rho_2)g+\frac{\mu_0}{h}\int_{-h/2}^{+h/2}dz\ M\ \frac{\partial}{\partial y}\left(\delta\psi+\zeta\frac{\partial\psi^0}{\partial y}\right)=0. \tag{7}$$

$\delta\psi$ is the variation of the magnetostatic potential due to the deformation of the free surface. Taking into account the kinematic boundary condition

$$\frac{\partial\zeta}{\partial t}=\frac{\partial\varphi_1}{\partial y}=\frac{\partial\varphi_2}{\partial y},$$

and the Laplace equation for the velocity potential $\Delta\varphi=0$, we obtain, for the Fourier amplitude of the periodic free-surface deformation ($\zeta=\zeta_k e^{ikx}$), the equation (k denotes the index of the Fourier component)

$$\frac{d\zeta_k}{dt}=\frac{k}{\alpha_1+\alpha_2}\left[-\sigma k^2\zeta_k-(\rho_1-\rho_2)g\zeta_k+\frac{\mu_0}{h}\int_{-h/2}^{+h/2}dz\ M\ \frac{\partial}{\partial y}\left(\delta\psi_k+\zeta\frac{\partial\psi_k^0}{\partial y}\right)\right]. \tag{8}$$

The variation of the magnetic field potential value $\delta\psi$ at $y=0$ is obtained by the expression

$$\psi=-\frac{1}{4\pi}\int_S d^2r'\ \frac{\vec{M}\cdot\vec{n}'}{|\vec{r}-\vec{r}'|}.$$

Integration along the free interface ($\vec{n}'$ is a unit vector normal to the interface) gives

$$\delta\psi=-\frac{1}{4\pi}\mathrm{P}\int_S dx'dz'\ \frac{My\zeta(x')}{[(x-x')^2+(z-z')^2]^{3/2}}$$

and

$$\frac{\partial\psi^0}{\partial y}=\frac{M}{4\pi}\mathrm{P}\int_S dx'dz'\ \frac{y}{[(x-x')^2+(z-z')^2]^{3/2}},$$

where P is the Cauchy principal value. Consequently, the following result:

$$\frac{\partial}{\partial y}\left(\delta\psi+\zeta\frac{\partial\psi^0}{\partial y}\right)=-\frac{1}{4\pi}\mathrm{P}\int_S dx'dz'\times\frac{M(\zeta(x')-\zeta(x))}{[(x-x')^2+(z-z')^2]^{3/2}}$$

and

$$\left[\frac{\partial}{\partial y}\left(\delta\psi_k+\zeta_k\frac{\partial\psi^0}{\partial y}\right)\right]_0=-\frac{M}{4\pi}\mathrm{P}\int_{-\infty}^{+\infty}dx\int_{-h/2}^{h/2}dz'\times\frac{e^{ik(x'-x)}-1}{[(x-x')^2+(z-z')^2]^{3/2}}.$$

As a result, the expression for the growth increment of the free-surface perturbations is given as ($\zeta_k\approx e^{\lambda(k)t}$)

$$\lambda(k)=\frac{k}{\alpha_1+\alpha_1}\left[-\sigma k^2-(\rho_1-\rho_2)g-\frac{\mu_0 M^2}{4\pi h}\int_{-h/2}^{h/2}dz\times\int_{-h/2}^{h/2}dz'\mathrm{P}\int_{-\infty}^{+\infty}dt\ \frac{e^{ikt}-1}{[t^2+(z-z')^2]^{3/2}}\right]. \tag{9}$$

The flat interface is unstable with respect to periodic deformations if $\lambda(k)$ becomes positive. This gives the following condition for the neutrality of the free-surface deformations:

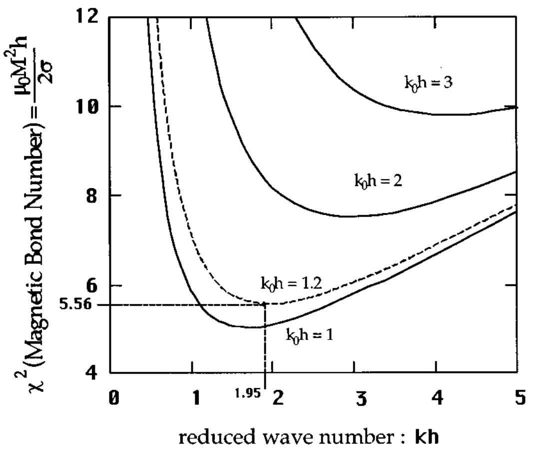

FIG. 2. Neutral curve for the 2D peak instability given $\chi^2 N_B = \mu_0 M^2 h/2\sigma$ as a function of the reduced wave number kh for different values of the reduced capillary wave number k_0h. $k_0h=1.2$ corresponds to the experimental result.

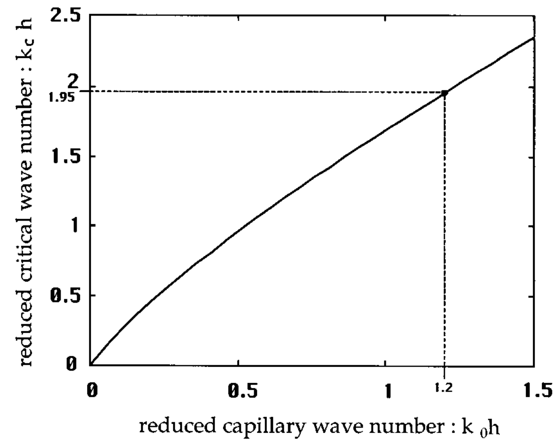

FIG. 3. Variation of $k_c h$ as a function of $k_0 h$. The measurement gives the reduced critical wave number $k_c h = 1.95$, which leads to the value of the reduced capillary wave number $k_0 h = 1.2$.

$$2\,\frac{\mu_0 M^2}{4\pi h}\,\mathrm{P}\int_{-\infty}^{+\infty} dt\;\frac{1-e^{ikt}}{t^2}\,\left(\sqrt{h^2+t^2}-|t|\right) = \sigma k^2 + (\rho_1-\rho_2)g. \tag{10}$$

Introducing the capillary wave vector $k_0 = 2\pi/\lambda_0$, Eq. (10) permits the determination of the critical magnetic Bond number as a function of the reduced wave number kh:

$$N_B\chi^2(H) = \frac{\mu_0 M^2 h}{2\sigma} = \frac{\pi}{2}\,\frac{(kh)^2+(k_0h)^2}{\int_0^{+\infty} dt\,\frac{1-\cos(t)}{t^2}\,\left[\sqrt{(kh)^2+t^2}-t\right]}. \tag{11}$$

The neutral curves determined by Eq. (11) for several values of k_0h are shown in Fig. 2. The instability corresponds to the minimum of the curve with a critical value $k_c h$. The dependence of $k_c h$ on $k_0 h$, obtained numerically according to relation (11), is shown in Fig. 3. On the basis of the data presented in Figs. 2 and 3, it is thus possible to obtain the value of σ from the measured value of $k_c h$.

B. Elongation of a magnetic droplet in flat layers

A MF droplet between two parallel walls (i.e., with a cylindrical symmetry), under the influence of a magnetic field normal to the layer, shows a wide variety of different equilibrium shapes [1,4]. The deformation of a droplet with a field tangential to the walls has been studied experimentally in Ref. [12]. It has been shown that the droplet shape becomes elliptical. In the present article, the elongation of the elliptical shape is calculated as a function of the external field H_0 and the surface tension σ. The rather complicated calculations may be simplified by the following assumption: the magnetization is constant and equal to that of the field strength acting on the center of the droplet. This seems to be reasonable since the demagnetizing factor is small in this case.

Let us consider a MF droplet of volume $V = \pi R^2 h$, where R is the initial radius of the circular boundary along the two walls. The system with its reference axes is sketched in Fig. 4. Since V and h are constant, the total surface along the two walls $2S = 2(\pi ab)$ is constant. Only the interface between the MF and the other liquid changes during the experiment. The general expression for the field strength due to the magnetization of the MF is written

$$\vec{H} = -\vec{\nabla}_r \int_{V-V_\varepsilon} d^3r'\;\frac{1}{4\pi}\,\frac{\vec{M}\cdot(\vec{r}-\vec{r}\,')}{|\vec{r}-\vec{r}\,'|^3}.$$

V_ϵ is a cutoff volume. We suppose now that the problem is invariant in the z direction and that the local field effects are negligible. Consequently, it can be expressed as

$$\vec{H} = -\frac{1}{4\pi}\,\vec{\nabla}_r \int_{S-S_\varepsilon} d^2r'\;\frac{\vec{M}\cdot\vec{n}\,'}{|\vec{r}-\vec{r}\,'|},$$

where the integration is along the interface of the droplet ($\vec{n}\,'$ is a unit vector perpendicular to the interface). The magnetic field strength at the center of the droplet can be expressed as

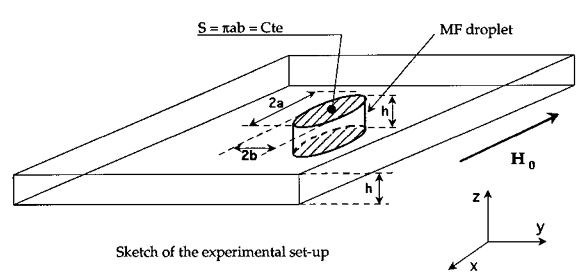

FIG. 4. Sketch of the Hele-Shaw cell in the MF droplet deformation experiment.

$$\vec{H}(\vec{0}) = -\frac{1}{4\pi}\int_S d^2r' \frac{\vec{M}\cdot\vec{n}'}{r'^3}\vec{r}'.$$

Focusing on the component along the external field after a simple integration along the surface of an elliptical cylinder (main axes a,b and height h), we have

$$H_x(0) = -\frac{Mhab}{\pi a^3}\frac{A}{e^2}[(e^2-1)\Pi(e^2,eA)+K(eA)], \tag{12}$$

where K and Π are the complete elliptical integrals of the first and third kind, e is the eccentricity defined by $e^2=1-b^2/a^2$, and A is the undimensional quantity $A^{-2}=1+(h/2a)^2$. Under our assumption, the magnetization of the droplet is determined by $M=\chi(H_0+H_x(0))$. Introducing a demagnetizing factor $D(e)$, which depends on e, we have $H_x(0)=-DM$. The magnetic energy of the droplet is

$$E_m = -\frac{\mu_0}{2}MH_0V = -\frac{\mu_0}{2}\frac{\chi H_0^2 V}{1+\chi D(e)}.$$

The total energy E_{total} of the MF droplet accounting for the surface energy can be expressed as

$$E_{\text{total}} = 4\sigma ahE(e) - \frac{\mu_0}{2}\frac{\chi H_0^2 V}{1+\chi D(e)}. \tag{13}$$

$E(e)$ is the complete elliptical integral of the second kind. The minimization the droplet energy E_{total} with respect to its eccentricity e, after simple but tedious calculations, gives the magnetic Bond number N_B,

$$N_B = \frac{h}{R}\frac{1}{e^2(1-e^2)^{1/4}}\frac{[1+\chi D(e)]^2}{-\pi\chi^2\frac{dD(e)}{de^2}}\left[\frac{2-e^2}{1-e^2}E(e)-2K(e)\right], \tag{14}$$

where the derivative of the demagnetizing factor with respect to the square eccentricity is expressed as

$$\frac{dD(e)}{de^2} = \frac{hR^2A}{\pi a^3 e^4}\left[\Pi(e^2,eA) - \frac{4-e^2}{4(1-e^2)}K(eA) + \frac{e^2}{4(1-e^2)}E(eA)\right].$$

It is also possible to derive, by an expansion of the total energy up to the first nonvanishing terms in small eccentricity, an approximate relation. This relation is valid for the small elongations of the droplet:

$$E_{\text{total}} \approx 2\pi\sigma hR\left[\frac{3e^4}{64} - \frac{1+2B^{-2}}{16(\chi\sqrt{B^{-2}-1}+2B^{-1})}\chi^2 BN_B e^2\right] + C^{te},$$

where B is given by $B^{-2}=1+(h/2R)^2$. For small eccentricities, we obtain as a function of the magnetic Bond number

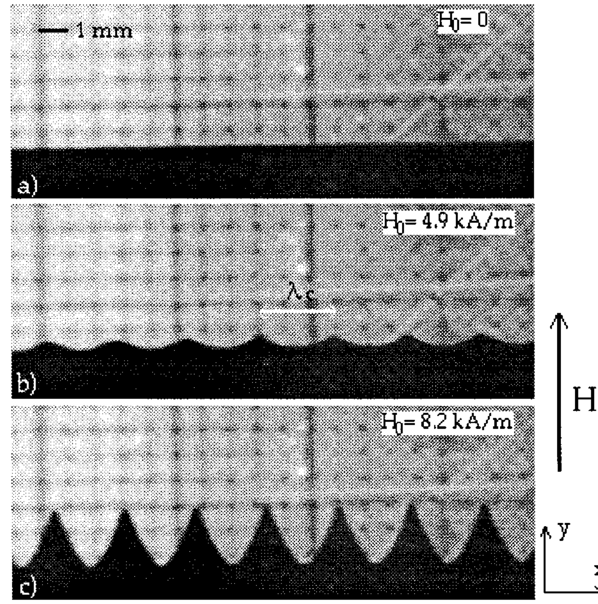

FIG. 5. Three photographs of the free MF-oil interface for different magnetic fields: (a) $H_0=0$, (b) $H_0=4.9$ kA m^{-1}, and (c) $H_0=8.2$ kA m^{-1}. The underlying millimetric grid gives the scale.

$$e^2 \approx \frac{2}{3}\frac{3+2(B^{-2}-1)}{\chi\sqrt{B^{-2}-1}+2B^{-1}}\chi^2 BN_B. \tag{15}$$

III. EXPERIMENTAL DESCRIPTION AND RESULTS

The same cell is used in both determinations of the surface tension. The external field H_0 is homogeneous and static.

A. Experimental setup

A MF (or ferrofluid) is a colloidal suspension of nanoscopic magnetic particles. Here we use an ionic (water-based) MF with cobalt ferrite particles ($CoFe_2O_4$) of mean size of roughly 10 nm [13]. The MF saturation magnetization is $M_s=40$ kA m^{-1}, with a particle volume fraction of 10%. The magnetic susceptibility is equal to $\chi_0=2.2\pm0.9$. The cell, sketched in Figs. 4 and 5, is made of two parallel sheets of Altuglas®; the distance between the two walls gives the cell thickness $h=0.9$ mm. This Hele-Shaw cell is filled with of an organic liquid (white spirit) and a small amount of MF. This MF is face to face with the organic liquid to avoid wetting of the MF along the two walls and to decrease the gravity effect by matching the density difference: MF: $\rho_1=1580$ kg m^{-3} and oil: $\rho_2=800$ kg m^{-3}.

An image processing is required to obtain the deformation of the MF-oil interface. The images are recorded by a charge coupled device camera and digitized by an acquisition card in a computer.

B. Spike instability: Results

Figure 5(a) shows a flat interface for $H_0=0$. Figure 5(b) shows the perturbed interface for a magnetic field value

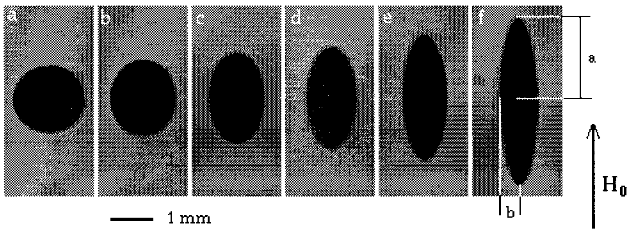

FIG. 6. Photographs of the MF droplet deformation for different tangential magnetic fields: (a) $H_0=0$, (b) $H_0=1.2$ kA m^{-1}, (c) $H_0=2.4$ kA m^{-1}, (d) $H_0=2.9$ kA m^{-1}, (e) $H_0=3.7$ kA m^{-1}, and (f) $H_0=5.5$ kA m^{-1}.

$H_0=4.9$ kA m^{-1} just above the threshold. The application of a field $H_0=8.2$ kA m^{-1} leads to the formation of a comb made of a single line of peaks, as shown in Fig. 5(c). Since $\chi<2.54$, the peak instability is a second-order transition [14]; this is confirmed here since no hysteresis is detected. The measured values of the wavelength and of the magnetic field at the threshold are $\lambda_c=2\pi/k_c=(2.89\pm0.07)$ mm and $H_c=(4.60\pm0.03)$ kA m^{-1}. If we neglect the demagnetizing factor, which is small here because H_0 is applied along the cell $D=(2/\pi)\tan^{-1}(h/l)\approx4\times10^{-2}$ (l is the MF height), the magnetization is given by $M_c=\chi(H_c)H_c/[1+D\chi(H_c)]\approx\chi(H_c)H_c\approx7.9$ kA m^{-1}. The curve in Fig. 3 gives $kh_0=1.2$ from $kh_c=1.95$. This leads to a value of the surface tension at the MF-oil interface: $\sigma=(3.89\pm0.04)$ mN m^{-1}. The value of M_c deduced from the Fig. 2 is $M_c=6.2$ kA m^{-1}, 20% less than the experimental result.

C. Droplet deformation: Results

The elliptical deformations of the MF droplet are shown in Fig. 6. The experimental results and the numerical calculation following (14) for the eccentricity e of the MF droplet are plotted as a function of the magnetic Bond number N_B in Fig. 7. The agreement between results allows the determination of the surface tension between the MF and oil at room temperature $\sigma=(3.07\pm0.04)$ mN m^{-1}.

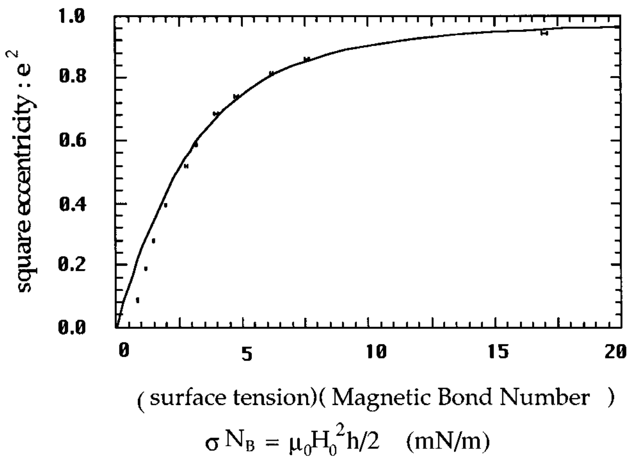

FIG. 7. Square eccentricity of the MF droplet ($e^2=1-b^2/a^2$) as a function of the product $\sigma N_B=\mu_0H_0^2h/2$: experimental points and exact calculation (continous line). Errors bars for σN_B are shown. The surface tension is determined by matching the experimental points by a least-squares method. Points of small eccentricities are disregarded due to the meniscus phenomena, which are not accounted for in the present model.

IV. DISCUSSION AND CONCLUSIONS

We present two general methods of measuring the surface tension between a magnetic liquid and another immiscible fluid. Despite the use of different approximations, the agreement between the two types of determination is good.

In the droplet deformation experiment, the hypothesis of a constant magnetization is a rather good approximation since the theoretical calculation fits quite well the experimental data. An important remark necessary to justify the Hele-Shaw approach in the peak instability experiment is that the effect of the confined geometry is not a correction: $k_c\approx2k_0$.

We can notice that a discrepancy between the calculation and the experimental data in the droplet experiment occurs for low values of the magnetic Bond number, i.e., below $N_B^*=\mu_0H_0^2R/2\sigma\approx1$, where R is the radius of the initial droplet. The reason of this shift could be capillary effects: because of the confined geometry we have taken a slice of an infinite system with a magnetization that is invariant perpendicularly to the walls. This basic hypothesis is only an approximation since a meniscus exists.

In the peak instability experiment the theoretical value of the magnetic field threshold H_c is lower than the experimental one. Here again we have postulated a 2D geometry and a magnetization that is homogeneous and the demagnetizing field is neglected in the first nonvanishing term obtained by linearization of the equations of the peak instability. Consequently, in the framework of these strong approximations, it is not so surprising that discrepancies occur even for magnetic Bond number $N_B^c=\mu_0H_0^2\lambda_c/2\sigma\approx12$, which is greater than N_B^*: it could be again capillary effects that are more sensitive here to the demagnetizing factor of the meniscus. Nevertheless, the two calculations give similar results for the determination of the surface tension, meaning that the essence of the physic is contained in our two models.

In the present work we assume that the surface tension is not dependent on the applied magnetic field. The autocoherence of our experimental results validates this hypothesis in the range of the magnetic fields used. For a more detailed description of the interface, further experiments, such as x-ray or neutron reflectivity, would be useful. It could detect, for example, structures of magnetic particles near the interface depending on the magnetic field direction (either parallel or perpendicular to the surface) or the formation of a depletion layer (or a concentrated layer) close to the interface.

ACKNOWLEDGMENTS

We are greatly indebted to P. Lepert for realization of the experimental setup. One of us (A.C.) thanks ''le Réseau Formation Recherche No. 90R0933 du MRES'' of France and ''International Science Foundation'' for financial support.

[1] A. Cebers and M. M. Maiorov, Magn. Gidrodin. **1**, 27 (1980).
[2] R. E. Rosensweig, M. Zahn, and R. Shumovich, J. Magn. Magn. Mater. **39**, 127 (1983).
[3] J.-C. Bacri, R. Perzynski, and D. Salin, Recherche **18**, 1150 (1987).
[4] S. A. Langer, R. E. Goldstein, and D. P. Jackson, Phys. Rev. A **46**, 4894 (1992).
[5] D. P. Jackson, R. E. Goldstein, and A. Cebers, Phys. Rev. E **50**, 298 (1994).
[6] A. Cebers, Magn. Gidrodin. **30**, 179 (1994).
[7] C. Flament, J.-C. Bacri, A. Cebers, F. Elias, and R. Perzynski, (to be published).
[8] G. L. Gaines, *Insoluble Monolayers at Liquid-Gas Interfaces* (Interscience, New York, 1966).
[9] J. Lucassen and R. S. Hansen, J. Colloid Interface Sci. **22**, 32 (1966).
[10] M. D. Cowley and R. E. Rosensweig, J. Fluid Mech. **30**, 671 (1967).
[11] J.-C. Bacri and D. Salin, J. Phys. Lett. **45**, 559 (1984).
[12] V. Bashtovoi *et al.*, (unpublished).
[13] S. Neveu-Prin, F. A. Tourinho, J.-C. Bacri, and R. Perzynski, Colloid Surf. A **80**, 1 (1993).
[14] V. M. Zaitsev and M. I. Shliomis, Proc. Acad. Sci. USSR **188**, 1261 (1969).